| | | |
|---|---|---|
| ESRF | **Experiment title:**<br>Advancing grain growth models for transparent alumina ceramics | **Experiment number**:<br>MA-5608 |
| **Beamline**:<br>ID11 | **Date of experiment**:<br>from: 09 July 2023 to: 17 July 2023 | **Date of report**:<br>10 Sep 2023 |
| **Shifts:**<br>18 | **Local contact(s)**:<br>Jon Wright, Wolfgang Ludwig | *Received at ESRF:* |

**Names and affiliations of applicants** (* indicates experimentalists):

Wenxi Li[1*], Celeste Perez[1*], Janice Moya[1*], Timothy Thompson[1*], Jon Wright[2], Wolfgang Ludwig[2], Ashley Bucsek[1*]

[1]University of Michigan; [2]ESRF

**Preliminary Report:**

Motivation: The goal of the experiment is to measure grain boundary velocity as a function of grain boundary character using scanning 3D X-ray diffraction (scanning 3DXRD) during in-situ sintering of alumina. There is a significant need for high quality anisotropic transparent ceramics such as alumina for next generation laser-host materials. To achieve transparent anisotropic alumina polycrystals, abnormal grain growth should be prevented during the sintering step to restrict the grain size below 1 μm. Grain growth is dictated by the growth rates of grain boundaries, which can vary due to anisotropy in surface energies. Understanding grain growth during the last stage of sintering as a function of anisotropic grain boundary energy through simulations informed by in-situ measurements is the motivation for this proposal. Because of the relatively small grain size (5–20 μm), scanning 3DXRD is indispensable, with spatial resolutions dictated by the beam cross-section (150–200 nm²) [1,2], to spatially resolve crystallographic orientations across the sample and measure grain boundary character and positions as a function of time. The results will be integrated into a novel computational methodology of grain growth using a Cauchy-Crofton/graph-based approach, and, more generally, develop a modern, predictive understanding of grain growth that takes into consideration the energies of different grain boundaries.

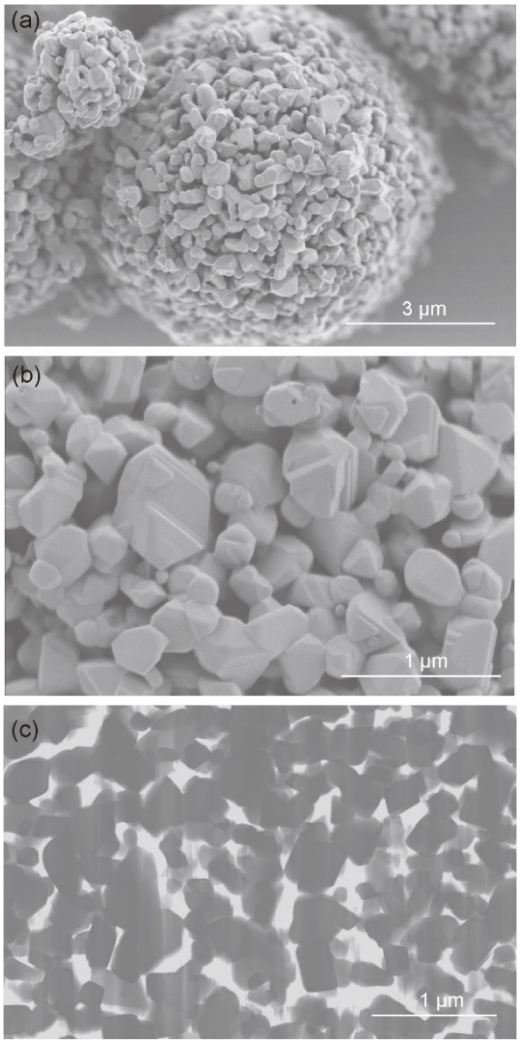


*Figure 1. SEM images of Alumina powder. (a) morphology of particle agglomerates (b) individual particle shape on the surface of agglomerates (c) distribution of cross-sectional porosity within an agglomerate.*

Experiment Overview: In this experiment, commercial alumina powder with>99.99% purity with average particle sizes of 300 nm was used to fabricate the bulk $Al_2O_3$ ceramic sample. The alumina powder was characterized at Michigan Center for Materials Characterization. Then, fully recrystallized anisotropic alumina samples were prepared and machined using FIB and transported to ID11 at the ESRF. In-situ phase contrast transmission (PCT), X-ray diffraction tomography (DCT), and scanning 3DXRD were performed on ID11. By combining the different modalities, we were able to characterize the microstructure evolution during grain growth

on different length scales, from the subgrain orientation of individual grains (using scanning 3DXRD) to the aggregate behavior of several thousands of grains (using PCT and DCT).

Results: Preliminary results are shown in **Fig. 1−3**. It is theoretically known that different sized spheres packed at random (with a broad size distribution) can lead to a packing ratio as high as 0.95 [3,4]. However, anisotropic crystals are of polyhedral shapes as shown in with high pore coordination numbers and packing density rarely reaches above 0.7 [5]. In the sintering of polycrystalline ceramics, it is essential to achieve a well-organized particle arrangement to reduce porosity and, consequently, attain the best optical properties. As a result, characterizing the powder's shape and pore distribution plays a crucial role in comprehending the sintering process. **Fig. 1** illustrates the initial characteristics of the alumina powder at the University of Michigan. In **Fig. 1(b)**, the initial particle shapes on the surface of the agglomerates from **Fig. 1(a)** are displayed. These particles are polyhedral and have sizes ranging from approximately 50 to 200 nm. To illustrate the porosity distribution, the agglomerates were sectioned using FIB. The porosity distribution spans from about 20 to 150 nm. These results will be used to inform the effect of particle shapes of on final product packing.

**Fig. 2** illustrates the PCT measurements of the bulk sample at various heating temperatures. In **Fig. 2(a)**, the initial microstructure exhibits a dispersed grain distribution and a rough surface. As the heating temperature rises to 1200 ℃, the porosity decreases, as shown in **Fig. 2(b)**. At a heating temperature of 1300 ℃, there is a prominent change in the microstructure, as shown in **Fig. 2(c)**. The porosity continues to decrease, and the sample surface becomes smoother, indicating grain growth at that temperature. The grain morphology and orientation distribution were measured using scanning 3DXRD after two heat treatments at 1300 ℃ for 5 minutes each.

**Fig. 3** illustrates the scanning 3DXRD measurements of a 2D layer in the bulk sample at various heating temperatures. **Fig. 3(a)** shows a preview of the spatially-resolved orientation map initial microstructure with grain color based on the crystal orientation shown in the inverse pole figure (IPF). **Fig. 3(b-c)** shows the spatially-resolved boundary positions as a function of heating time. Notice that the local microstructure exhibits varying growth behavior. As the heating temperature increases, the number of grains in the 2D layer decreases from 118 to 88, indicating the grain coarsening process during heat treatment.

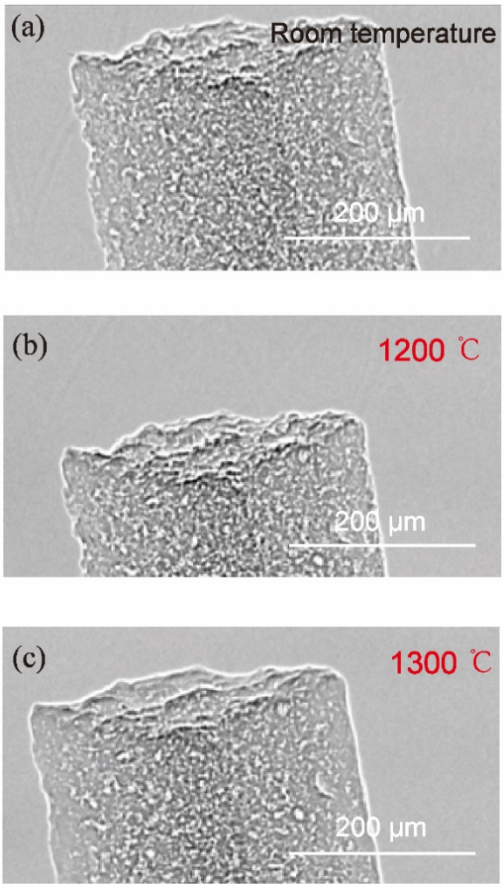


*Figure 2. Preliminary results: (a) PCT measurement of the initial microstructure. (b) PCT measurement at the heating temperature of 1200 ℃ (c) PCT measurement at the heating temperature of 1300 ℃.*

Current and Future Plans: The results presented above are preliminary. Currently, we are analyzing the PCT and scanning 3DXRD data, as well as the DCT data, culminating in the ability to investigate the microstructural evolution of the bulk samples at different heating temperatures across multiple length scales. The PCT data will yield information about the 3D porosity distribution and pore evolution within the bulk sample. The DCT data will provide a 3D view of all the grains in the bulk sample, which can be used to validate the scanning 3DXRD measurements (Note: Some grain information may be missing due to the small grain size in the initial microstructure). The scanning 3DXRD data will be employed to reconstruct the 3D grain morphology by stacking the 2D layers together. Thanks to its high spatial resolution (250 nm in this experiment), the scanning 3DXRD data can also offer subgrain-level orientation and local grain boundary details for each grain throughout the heat treatment process. Lastly, we will develop a new 3D grain topology processing pipeline to automatically measure grain boundary curvature and detect grain triple points, as well as quadruple points for bulk sample.

Finally, future work will involve the integration of 2D layer information into 3D data, enabling us to track individual grain boundary positions, local orientation evolution, and the measurement of grain boundary character in 3D as a function of time. The results will be used to inform a novel computational methodology of grain growth using a Cauchy-Crofton/graph-based approach, and, more generally, develop a modern, predictive understanding of grain growth that takes into consideration the anisotropic energies of different grain

boundaries. Building upon the technique developed during this PCT+ scanning 3DXRD+DCT experiment at ID11 on anisotropic Alumina, our goal is to apply this approach to the investigation of other ceramic materials in a future beamtime proposal.

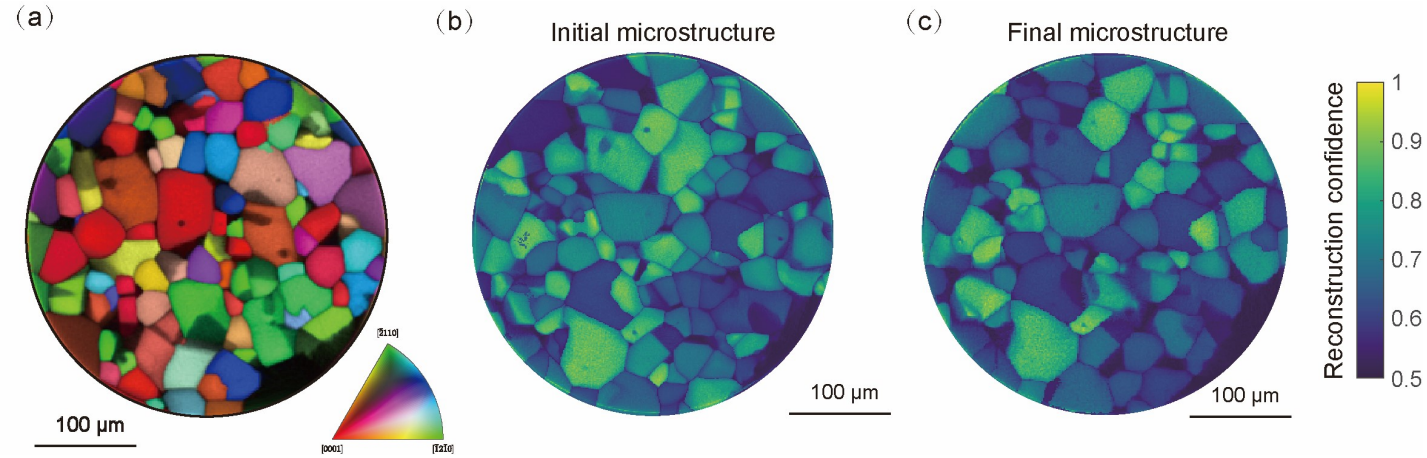


*Figure 3. Preliminary results: (a) The initial microstructure colored by orientation given by the IPF. (b) Reconstruction confidence map of initial microstructure. (c) Reconstruction confidence map of final microstructure.*

References:


[1] N.A. Henningsson, S.A. Hall, J.P. Wright, J. Hektor, Reconstructing intragranular strain fields in polycrystalline materials from scanning 3DXRD data, J Appl Cryst. 53 (2020) 314–325. https://doi.org/10.1107/S1600576720001016.

[2] J. Hektor, S.A. Hall, N.A. Henningsson, J. Engqvist, M. Ristinmaa, F. Lenrick, J.P. Wright, Scanning 3DXRD Measurement of Grain Growth, Stress, and Formation of Cu6Sn5 around a Tin Whisker during Heat Treatment, Materials. 12 (2019) 446. https://doi.org/10.3390/ma12030446.

[3] J. Ma, L.C. Lim, Effect of particle size distribution on sintering of agglomerate-free submicron alumina powder compacts, Journal of the European Ceramic Society. 22 (2002) 2197–2208. https://doi.org/10.1016/S0955-2219(02)00009-2.

[4] R.M. German, S.J. Park, Handbook of Mathematical Relations in Particulate Materials Processing: Ceramics, Powder Metals, Cermets, Carbides, Hard Materials, and Minerals, John Wiley & Sons, 2009.

[5] J. Zheng, J.S. Reed, Effects of Particle Packing Characteristics on Solid-State Sintering, Journal of the American Ceramic Society. 72 (1989) 810–817. https://doi.org/10.1111/j.1151-2916.1989.tb06222.x.